8822 *Inorg. Chem.* **2009**, *48*, 8822–8829
DOI: 10.1021/ic901000d

Inorganic Chemistry
Article

Magnetic Circular Dichroism Study of a Dicobalt(II) Complex with Mixed 5- and 6-Coordination: A Spectroscopic Model for Dicobalt(II) Hydrolases

James A. Larrabee,* W. Rainey Johnson, and Adam S. Volwiler

Department of Chemistry and Biochemistry Middlebury College Middlebury, Vermont 05753

Received May 22, 2009

The magnetic circular dichroism (MCD) study of [Co_2(μ-OH)(μ-Ph_4DBA)(TMEDA)$_2$(OTf)], in which Ph_4DBA is the dinucleating bis(carboxylate) ligand dibenzofuran-4,6-bis(diphenylacetate) and TMEDA is *N*,*N*,*N*′,*N*′-tetramethylethylenediamine, is presented. This complex serves as an excellent spectroscopic model for a number of dicobalt(II) enzymes and proteins that have both the μ-hydroxo, μ-carboxylato bridging and asymmetric 6- and 5-coordination. The low-temperature MCD spectrum of the model complex shows bands at 490, 504, and 934 nm arising from d-d transitions on the 6-coordinate Co^{II} and bands at 471, 522, 572, 594, and 638 nm arising from d-d transitions on the 5-coordinate Co^{II}. The most intense MCD bands are at 504 and 572 nm for 6- and 5-coordinate Co^{II}, respectively, and these two bands are found in the MCD spectra of dicobalt(II)-substituted methionine aminopeptidase from *Escherichia coli* (CoCoMetAP), glycerophosphodiesterase from *Enterobacter aerogenes* (CoCoGpdQ), aminopeptidase from *Aeromonas proteolytica* (CoCoAAP), and myohemerythrin from *Themiste zostericola* (CoCoMyoHry). These dicobalt(II)-substituted proteins are known to have one 5- and one 6-coordinate Co^{II} bridged by one or two carboxylates and either a water or a hydroxide. The uncertainty of the bridging water's state of protonation is problematic, as this is a likely candidate for the attacking nucleophile in the dimetallohydrolases. Analysis of the variable-temperature variable-field (VTVH) MCD data determined that the Co^{II} ions in the model complex are ferromagnetically coupled with a J of 3.0 cm^{-1}. A comparison of all dicobalt(II) complexes and dicobalt(II)-substituted protein active sites with the μ-hydroxo/aqua, μ-carboxylato bridging motif reveals that J is either zero or negative (antiferromagnetic) in the μ-aqua systems and positive (ferromagnetic) in the μ-hydroxo systems. It was also determined that the Co^{II} ions in CoCoAAP and CoCoMyoHry are ferromagnetically coupled, each with a J of 3.4 cm^{-1}, which suggests that these ions have a μ-hydroxo bridging ligand.

Introduction

A remarkable number of functionally diverse metalloproteins share the μ-hydroxo (or μ-aqua), μ-carboxylato dimetal(II) active site structural motif.[1−3] Examples include the dioxygen binding protein hemerythrin (Hry) found in some marine invertebrates,[4] the ubiquitous *N*-terminal methionine aminopeptidase (MetAP),[1] an aminopeptidase found in *Aeromonas proteolytica* (AAP),[3] a glycerophosphodiesterase from *Enterobacter aerogenes* (GpdQ),[5,6] and phosphotriesterases from *Agrobacterium radiobacter* (OpdA)[7] and *Pseudomonas diminuta* (PTE).[8] X-ray crystallographic studies have shown that OpdA has two 6-coordinate metal binding sites and PTE has two 5-coordinate binding sites. AAP has either two 5-coordinate or one 5- and one 6-coordinate binding site (for cobalt), and Hry, MetAP, and GpdQ have one 6-coordinate and one 5-coordinate metal binding site (Chart 1). In MetAP, only the 5-coordinate site is fully occupied at low metal concentration, leading many investigators to the conclusion that it is a monometallic hydrolase.[9−11] On the other hand, the 6-coordinate site has the higher metal binding affinity in GpdQ, but the presence of substrate causes the 5-coordinate

*To whom correspondence should be addressed. E-mail: larrabee@middlebury.edu.

(1) Lowther, W. T.; Matthews, B. M. *Chem. Rev.* **2002**, *102*, 4581–4607.
(2) Mitić, N.; Smith, S. J.; Neves, A.; Guddat, L. W.; Gahan, L. R.; Schenk, G. *Chem. Rev.* **2006**, *106*, 3338–3363.
(3) Holz, R. C. *Coord. Chem. Rev.* **2002**, *232*, 5–26.
(4) Holmes, M. A.; LeTrong, I.; Turley, S.; Sieker, L. C.; Stenkamp, R. E. *J. Mol. Biol.* **1991**, *218*, 583–593.
(5) Jackson, C. J.; Carr, P. D.; Liu, J.-W.; Watt, S. J.; Beck, J. L.; Ollis, D. L. *J. Mol. Biol.* **2007**, *367*, 1047–1062.
(6) Hadler, K. S.; Tanifum, E.; Yip, S. H.-C.; Mitic, N.; Guddat, L. W.; Jackson, C. J.; Gahan, L. R.; Carr, P.; Ollis, D. L.; Hengge, A. C.; Larrabee, J. A.; Schenk, G. *J. Am. Chem. Soc.* **2008**, *130*, 14129–14138.
(7) Jackson, C.; Kim, H.-K.; Carr, P. D.; Liu, J.-W.; Beck, J. L.; Ollis, D. L. *Biochim. Biophys. Acta* **2005**, *1752*, 56–64.
(8) Benning, M. M.; Shim, H.; Raushel, F. M.; Holden, H. M. *Biochemistry* **2001**, *40*, 2712–2722.
(9) D'souza, V. M.; Bennett, B.; Copik, A. J.; Holz, R. C. *Biochemistry* **2000**, *39*, 3817–3826.
(10) D'souza, V. M.; Swierczek, S. I.; Cosper, N. J.; Meng, L.; Ruebush, S.; Copik, A. J.; Scott, R. A.; Holz, R. C. *Biochemistry* **2002**, *41*, 13096–13105.
(11) Ye, Q.-Z.; Xie, S.-X.; Ma, Z.-Q.; Huang, M.; Hanzlik, R. P. *Proc. Natl. Acad. Sci. U.S.A.* **2006**, *103*, 9470–9475.

 Published on Web 08/19/2009

Chart 1. Schematic Structures of Protein Active Sites That Have Asymmetric 6/5 Coordination

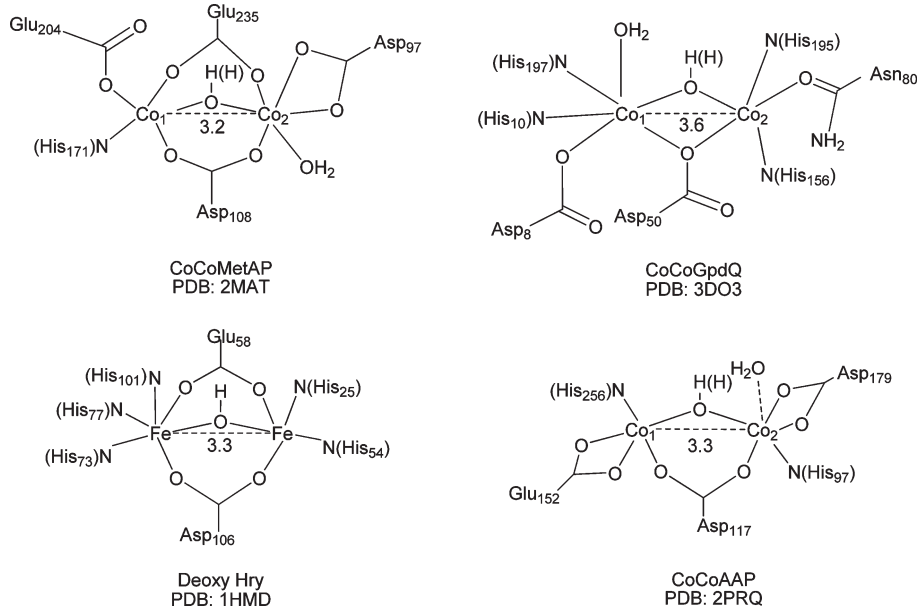

site to bind a metal, and only then does the enzyme become active.[6]

In cases in which solvent water may provide a ligand, determining the exact coordination number of metal ions in enzyme active sites through X-ray crystallography is not always possible. Furthermore, when binding affinities differ, crystallography may not be able to determine the higher affinity site. This is where spectroscopic studies are useful. Our understanding of MetAP and GpdQ has been advanced by magnetic circular dichroism (MCD) spectroscopic studies of the Co(II) versions.[6,12,13] Co(II) is a nearly ideal MCD spectroscopic probe metal, for a number of reasons. First, the dicobalt(II) forms of these enzymes are isostructural with the in vivo metal candidate forms: Mn(II) or Fe(II) for MetAP[11] and Zn(II) for GpdQ.[5] The actual in vivo metals for these enzymes are not known with certainty. In human MetAP, Mn(II) is a likely candidate,[14] and in bacterial MetAP, Fe(II)[15,16] or Mn(II)[10] are likely candidates. Second, the more intense d-d transitions from high-spin Co(II) are found in the visible wavelength region, and the energy of these transitions is diagnostic for 4-, 5-, and 6-coordination.[17,18] Third, high-spin Co(II) has a spin quartet ground state that yields temperature-dependent C-term MCD, which is very intense at low temperatures. The d-d transitions in the MCD spectrum are often observable in samples in which no visible absorption can be detected.[18] Finally, detailed analysis of the variable-temperature, variable-field (VTVH) MCD intensity data of dicobalt(II)-substituted enzymes can yield ground-state electronic parameters such as the magnetic exchange coupling constant, J, which is sensitive to subtle changes in the active site, particularly in the bridging ligand.[13,19−24]

Thus it is important to study the MCD spectra of small structural analogues of the μ- hydroxo(aqua), μ-carboxylato dicobalt(II) enzyme active sites to help interpret future results. Several dicobalt(II) complexes have been reported to have this bridging core structure.[13,25−31] However, these complexes differ in significant ways from the active-site structures in MetAP, GpdQ, Hry, and AAP. The most important difference is that both cobalt ions in the previously studied model complexes are 6-coordinate. A second difference is that the Co···Co distances in these complexes are between 3.44 and 3.69 Å, which causes the Co−O−Co angles to range from 113° to 121°. These distances are close to those of the GpdQ structure but far from those of the MetAP, Hry, and AAP structures, which have metal ion separations between 3.2 and 3.3 Å (Chart 1). The metal separation will affect the angle of the monatomic bridging ligand, which in turn may be an important influence on the magnitude of J.

(12) Larrabee, J. A.; Leung, C.-H.; Moore, R. L.; Thamrong-nawasawat, T.; Wessler, B. S. H. *J. Am. Chem. Soc.* **2004**, *126*, 12316–12324.
(13) Larrabee, J. A.; Chyun, S.-A.; Volwiler, A. S. *Inorg. Chem.* **2008**, *47*, 10499–10508.
(14) Wang, J.; Sheppard, G. S.; Lou, P.; Kawai, M.; Park, C.; Egan, D. A.; Schneider, A.; Bouska, J.; Lesniewski, R.; Henkin *J. Biochem.* **2003**, *42*, 5035–5042.
(15) D'souza, V. M.; Holz, R. C. *Biochemistry* **1999**, *38*, 11079–11085.
(16) Wang, W.-L.; Chai, S. C.; Huang, M.; He, H.-Z.; Hurley, T. D.; Ye, Q.-Z. *J. Med. Chem.* **2008**, *51*, 6110–6120.
(17) Kaden, T. A.; Holmquist, B.; Vallee, B. L. *Inorg. Chem.* **1974**, *13*, 2585–2590.
(18) Larrabee, J. A.; Alessi, C. M.; Asiedu, E. T.; Cook, J. O.; Hoerning, K. R.; Klingler, L. J.; Okin, G. S.; Santee, S. G.; Volkert, T. L. *J. Am. Chem. Soc.* **1997**, *119*, 4182–4196.
(19) Reem, R. C.; Solomon, E. I. *J. Am. Chem. Soc.* **1987**, *109*, 1216–1226.
(20) Solomon, E. I.; Pavel, E. G.; Loeb, K. E.; Campochiaro, C. *Coord. Chem. Rev.* **1995**, *144*, 369–460.
(21) Neese, F.; Solomon, E. I. *Inorg. Chem.* **1999**, *38*, 1847–1865.
(22) Strand, K. R.; Yang, Y.-S.; Andersson, K. K.; Solomon, E. I. *Biochemistry* **2003**, *42*, 12223–12234.
(23) Wei, P.; Skulan, A. J.; Mitić, N.; Yang, Y.-S.; Saleh, L.; Bollinger, J. M.; Solomon, E. I. *J. Am. Chem. Soc.* **2004**, *126*, 3777–3788.
(24) Wei, P.; Tomter, A. B.; Røhr, A. K.; Andersson, K. K.; Solomon, E. I. *Biochemistry* **2006**, *45*, 14043–14051.
(25) Coucouvanis, D.; Reynolds, R. A.; Dunham, W. R. *J. Am. Chem. Soc.* **1995**, *117*, 7570–7571.
(26) Schultz, B. E.; Ye, B.-H.; Li, X.; Chan, S. I. *Inorg. Chem.* **1997**, *36*, 2617–2622.
(27) Ye, B.-H.; Chen, X.-M. *Chin. J. Chem.* **2003**, *21*, 531–536.
(28) Brown, D. A.; Errington, W.; Glass, W. K.; Haase, W.; Kemp, T. J.; Nimir, H.; Ostrovsky, S. M.; Werner, R. *Inorg. Chem.* **2001**, *40*, 5962–5971.
(29) Turpeinen, U.; Ahlgren, M.; Hamalainen, R. *Acta Crystallogr.* **1982**, *B38*, 1580–1583.
(30) Turpeinen, U.; Hamalainen, R.; Reedijk, J. *Polyhedron* **1987**, *6*, 1603–1610.
(31) Chaudhuri, P.; Querbach, J.; Wieghardt, K.; Nuber, B.; Weiss, J. *J. Chem. Soc., Dalton Trans.* **1990**, 271–278.

Chart 2. Schematic Structure of the Model Complex

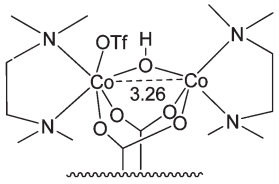

$[Co_2(\mu\text{-OH})(\mu\text{-Ph}_4\text{DBA})(\text{TMEDA})_2(\text{OTf})]$

OTf = triflate
TMEDA = N,N,N',N'-tetramethylethylenediamine
H_2Ph_4DBA =

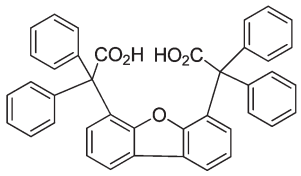

For these reasons, we have undertaken the MCD study of $[Co_2(\mu\text{-OH})(\mu\text{-Ph}_4\text{DBA})(\text{TMEDA})_2(\text{OTf})]$, in which Ph_4DBA is the dinucleating bis(carboxylate) ligand dibenzofuran-4,6-bis(diphenylacetate) and TMEDA is *N*,*N*,*N*′,*N*′-tetramethylethylenediamine (Chart 2).[32] This complex is unique, in that it has both the μ-hydroxo, bis(μ-carboxylato) bridging structure and the 6/5 asymmetric coordination. Furthermore, the Co···Co distance is a short 3.26 Å, and the Co−O−Co angle is small at 104°. This complex and the diiron(II) version were originally reported by Lippard et al., as structural and functional models of Co(II)-substituted Hry and native Hry, respectively.[32]

Experimental Section

Complex Preparation. The complex was prepared as previously described by Lippard et al.[32] except that the final assembly of the complex was done in a Vacuum Atmospheres glovebox with an oxygen level maintained below 1 ppm. The solvents used in recrystallization were degassed by the freeze−pump−thaw method. These precautions were taken because we noted that the complex was slightly air sensitive when in solution. Correct composition of the complex was confirmed by elemental analysis.

Spectroscopy. UV/vis/NIR absorption spectra were recorded with a Cary model 6000i spectrometer using a 50/50 (v/v) mixture of methylene chloride/toluene. Samples were loaded in a glovebox into screw-cap cuvettes. Diffuse reflectance spectra were recorded as a mixture of MgO powder on the Cary 6000i using a Harrick Praying Mantis Diffuse Reflectance Accessory. Precautions against air oxidation were not necessary because the samples were in the solid state.

Fresh samples were prepared before MCD data were collected. MCD samples were dissolved in a 50/50 (v/v) mixture of methylene chloride/toluene that was degassed by the freeze−pump−thaw method. The MCD sample cell (previously described) was loaded inside a glovebox and then placed directly into the SM4000 cryostat/magnet.[12] The MCD system used has a JASCO J815 spectropolarimeter and an Oxford Instruments SM4000 cryostat/magnet. Three separate sample preparations were conducted to collect VTVH MCD data. Data were collected at increments of 0.5 Tesla (T) from 0 to 7.0 T and at temperatures of 1.3, 3.0, 4.2, 6.0, 10, 20, and 50 K. Each spectrum was corrected by subtracting the zero-field spectrum of the sample. The instrument baseline has a very small deviation from zero (±0−5 millidegrees) that is both field- and wavelength-dependent. Each spectrum was corrected for the instrument baseline by subtracting a spectrum recorded at the same magnetic field but with no sample present. Finally, each spectrum was fitted to the minimum number of Gaussian peaks using the GRAMS/AI software to achieve a satisfactory composite spectrum. The absolute values of the heights of each Gaussian peak were used in the VTVH MCD data analysis.

A UV/vis absorption spectrum of the frozen glass was also generated from the photomultiplier tube high-voltage signal of the J815 spectropolarimeter. The high-voltage signal with no sample present was used as a reference.

Angular Overlap Model Calculations. Angular overlap model (AOM) calculations were made using AOMX, a program developed and distributed by Adamsky and co-workers.[33] AOMX determines the optimum ligand field parameters needed to fit an observed set of d-d transitions, based on a given structure. Input to AOMX requires the ligand coordinates referred to the metal ion at the origin. The coordinates were generated, using ChemDraw 3D, from the published bond angles and distances.[32] AOMX does not use the bond distances; only the angles are important, and they are fixed by the crystal structure. However, the bond distances are reflected by the magnitude of the resulting ligand field parameters, ε_σ and ε_π. Each Co^{II} metal site was treated separately. The values for r, θ, and φ for each metal ion are given in Supporting Information, Table S1.

The 5-coordinate site has a nearly trigonal bipyramidal shape, with one TMEDA nitrogen and one bridging carboxylate oxygen on the axial positions. To minimize the number of parameters, π-bonding was assumed to be negligible, and ε_σ for identical ligands was assumed to be proportional to $1/r^5$, where r is the bond length.[34] Thus ε_σ for the TMEDA nitrogen having the longer Co−N bond was calculated from ε_σ for the shorter TMEDA Co−N bond, which was allowed to float, according to: $\varepsilon_{\sigma(\text{long})} = \varepsilon_{\sigma(\text{short})}[r^5_{\text{Co-N(short)}}/r^5_{\text{Co-N(long)}}]$. Referring to Supporting Information, Table S1, 5-coordinate $r_{\text{Co-N(short)}}$ equals 2.1161 Å and the $r_{\text{Co-N(long)}}$ equals 2.2770 Å; thus, $\varepsilon_{\sigma(\text{long})} = \varepsilon_{\sigma(\text{short})}[0.693]$.

The 6-coordinate site has a distorted octahedral shape, with five of the six ligands identical to those of the 5-coordinate Co^{II}. The sixth ligand is the triflate oxygen. Because only three bands were observed, the ε_σ values obtained from the AOMX fit of the 5-coordinate Co^{II} bands were used in the AOMX fit of the 6-coordinate Co^{II} data after correction for bond distance using the $1/r^5$ dependence.

MCD Data Analysis. VTVH MCD data were normalized to the maximum observed intensity and were fitted using a Simplex algorithm that minimizes a chi-squared goodness of fit parameter. Two complementary models, a dimer model and a singlets/doublets model, were used in fitting the data for magnetically coupled $Co^{II}Co^{II}$ non-Kramers systems. In the dimer model, wave functions are calculated using a spin Hamiltonian (Equation S1 in Supporting Information), and the MCD intensity is given by the spin expectation values of the Co^{II} ion

(32) Mizoguchi, T. J.; Kuzelka, J.; Spingler, B.; DuBois, J. L.; Davydov, R. M.; Hedman, B.; Hodgson, K. O.; Lippard, S. J. *Inorg. Chem.* **2001**, *40*, 4662–4673.

(33) (a) Schonherr, T.; Atanasov, M.; Adamsky, H. *Comprehensive Coordination Chemistry II*; Lever, A. B. P., Ed.; Elsevier: Amsterdam, 2004; Vol. *2*, pp 443−455. (b) Adamsky, H.; Schonherr, T.; Atanasov, M. *Comprehensive Coordination Chemistry II*; Lever, A. B. P., Ed.; Elsevier: Amsterdam, 2004; Vol. *2*, pp 661−664. (c) Available on the internet at http://www.aomx.de. (d) Sakiyama, H.; Watanabe, Y.; Ito, R.; Nishida, Y. *Inorg. Chim. Acta* **2004**, *357*, 4309–4312. (e) Bencini, A.; Benelli, C.; Gatteschi, D. *Coord. Chem. Rev.* **1984**, *60*, 131–169.

(34) Lever, A. B. P.; Walker, I. M.; McCarthy, P. J.; Mertes, K. B.; Jircitano, A.; Sheldon, R. *Inorg. Chem.* **1983**, *22*, 2252–2258.

responsible for the MCD transition. The dimer model yields the coupling constant, J; the single ion zero-field splitting parameters, D and E; the polarization of the transition; and the energies and total M_s values of the resulting wave functions. For two high-spin Co^{II} ions, the dimer model yields 16 sublevels. The second fitting procedure uses a singlets/doublets model for non-Kramers (integral spin) or Kramers (non-integral spin) systems that includes an orientation-averaged MCD intensity expression, allowing for linear B-terms from field-induced mixing between states and the presence of thermally populated sublevels above the ground state (Equation S2 in Supporting Information). The singlets/doublets model yields the effective g for each doublet, the zero-field splitting in the dimer (non-Kramers system), δ, the energy of each level, and the M_z/M_{xy} polarization ratio. A third fitting procedure uses a monomer model for isolated (uncoupled) Co^{II} in which the MCD intensity is calculated just as it is in the dimer model, except the spin Hamiltonian includes only one metal and does not include a coupling term ($-2JS_1 \cdot S_2$ in Equation S1). The models, theory, equations, and computer programs to fit the VTVH MCD data have been developed by the Solomon group over the past several years and are described in detail elsewhere.[19−24] The computer programs and instructions for using them were kindly provided by the Solomon group.

Fitting VTVH MCD data from a coupled ($J \neq 0$) system using these two models/programs is an iterative process because the energy and total M_s of each sublevel given by the dimer model must be consistent with the energy and effective g given by the singlets/doublets model. Excellent descriptions of this process for coupled diiron(II) systems have been published.[23,24] In the coupled dicobalt(II) system described in this study, and in previous studies on an antiferromagnetically coupled dicobalt(II) complex[35] and a ferromagnetically coupled dicobalt(II) complex,[13] we found that it was better to fit the data to the dimer model first and then determine which energy levels would be populated at low temperatures and what the total M_s was for each of these levels. The energy and appropriate effective g were then set as a starting point when fitting the data using the singlets/doublets program. The VTVH MCD data sets that were fitted included all temperatures, nominally 1.3, 3.0, 4.2, 6, 10, 20, and 50 K; however, only three isotherms (at 1.3, 4.2, and 12.6 K) are shown in figures for clarity.

Results

Spectroscopy. Figure 1 shows the MCD spectrum and absorption spectrum of the complex at 1.3 K and 7.0 T. All the peaks in the MCD spectrum are temperature dependent C-terms, as is evident from their increasing intensity behavior as temperature is lowered (Supporting Information, Figure S1). The absorption spectrum of the frozen glass at 1.3 K is similar to the absorption spectrum of the dichloromethane/toluene solution spectrum at room temperature (data not shown). The MCD and absorption spectra in the frozen glass are very similar, except for signal-to-noise, to the MCD spectrum of the solid mull and the diffuse reflectance spectrum (Supporting Information, Figure S2). This observation confirms that the structure of the solid is left intact in solution.

The MCD spectrum is far better resolved than is the absorption spectrum. Therefore, the MCD spectrum was used to establish the minimum number of band centers arising from d-d transitions on the two Co^{II} centers. The 7 T MCD spectra taken at 1.3, 4.2, 12.6, 26.7, and 50.0 K were fitted to the minimum number of Gaussian peaks using the Grams/AI software. In all cases, the minimum number of Gaussian peaks necessary to achieve a good fit was seven, centered at 471(−), 490(+), 504(−), 522(−), 572(−), 594(+), and 638(+) nm. In addition to these peaks, the near-infrared MCD spectrum showed a very broad, weak peak centered at 934(+) nm, which was observed in the room-temperature absorption and diffuse reflectance spectra at 1064 nm (data not shown). These Gaussian peaks are shown in red in Figure 1. The composite MCD spectrum is indistinguishable from the experimental spectrum except for the noise.

Gaussian fitting of the low-temperature or the room-temperature absorption spectra did not result in an unequivocal solution. This is partly due to the quality of the absorption spectrum caused by poor resolution, overlapping ligand absorptions, light scattering from the frozen glass, and baseline uncertainty. However, the absorption spectrum could be satisfactorily fit to

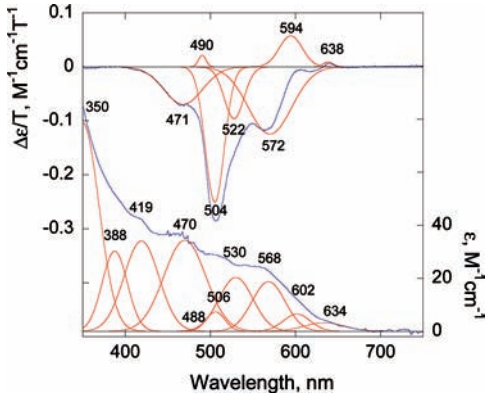

Figure 1. MCD (top) and absorption spectrum (bottom) of model complex in 50/50 methylene chloride/toluene at 1.3 K and 7.0 T. The blue lines are the experimental spectra, and the red lines represent the best fit Gaussian peaks.

Table 1. Vis/NIR, MCD, and AOM Calculations for $[Co_2(\mu\text{-OH})(\mu\text{-Ph}_4\text{DBA})(\text{TMEDA})_2(\text{OTf})]$

Vis/NIR[a] λ_{max} [nm] (ε) [M^{-1} cm^{-1}]	MCD[b] λ_{max} [nm] ($\Delta\varepsilon/T$) [M^{-1} cm^{-1} T^{-1}]	calcd[c]	origin of d-d in D_{3h}
	5-C Co^{II}		
634 (3.2)	638 (+0.009)	634	$^4A'_2 \rightarrow {}^4E'$
602 (6.5)	594 (+0.057)	609	
568 (18.7)	572 (−0.13)	567	$^4A'_2 \rightarrow {}^4A'_2(P)$
530 (20.3)	522 (−0.096)	521	$^4A'_2 \rightarrow {}^4E''$ (P)
470 (34.3)	471 (−0.070)	469	
Vis/NIR[a] λ_{max} [nm] (ε) [M^{-1} cm^{-1}]	MCD[b] λ_{max} [nm] ($\Delta\varepsilon/T$) [M^{-1} cm^{-1} T^{-1}]	calcd[c]	origin of d-d in O_h
	6-C Co^{II}		
1064[d]	934 (+0.01)	1004	$^4T_{1g} \rightarrow {}^4T_{2g}$
506 (7.3)	504 (−0.25)	504	$^4T_{1g} \rightarrow {}^4T_{1g}(P)$
488 (0.003)	490 (+0.02)	460	

[a] In 50/50 methylene chloride/toluene glass at 1.3 K. [b] In 50/50 methylene chloride/toluene glass at 1.3 K and 7 T. [c] AOMX parameters (cm^{-1}) 5-C Co^{II}: ε_σ(tmedaN) = 8620, 5970; $\varepsilon_\sigma(OH^-)$ = 6500; ε_σ(carboxylateO) = 2940, 2280; B = 494. AOMX parameters (cm^{-1}) 6-C Co^{II}: ε_σ(tmedaN) = 6800, 6600; $\varepsilon_\sigma(OH^-)$ = 4530; ε_σ(carboxylateO) = 2350, 2160; ε_σ(triflateO) = 1220; B = 670. [d] From diffuse reflectance spectrum.

(35) Johansson, F. B.; Bond, A. D.; Nielsen, U. G.; Moubaraki, B.; Murray, K. S.; Berry, K. J.; Larrabee, J. A.; McKenzie, C. J. *Inorg. Chem.* **2008**, *47*, 5079–5092.

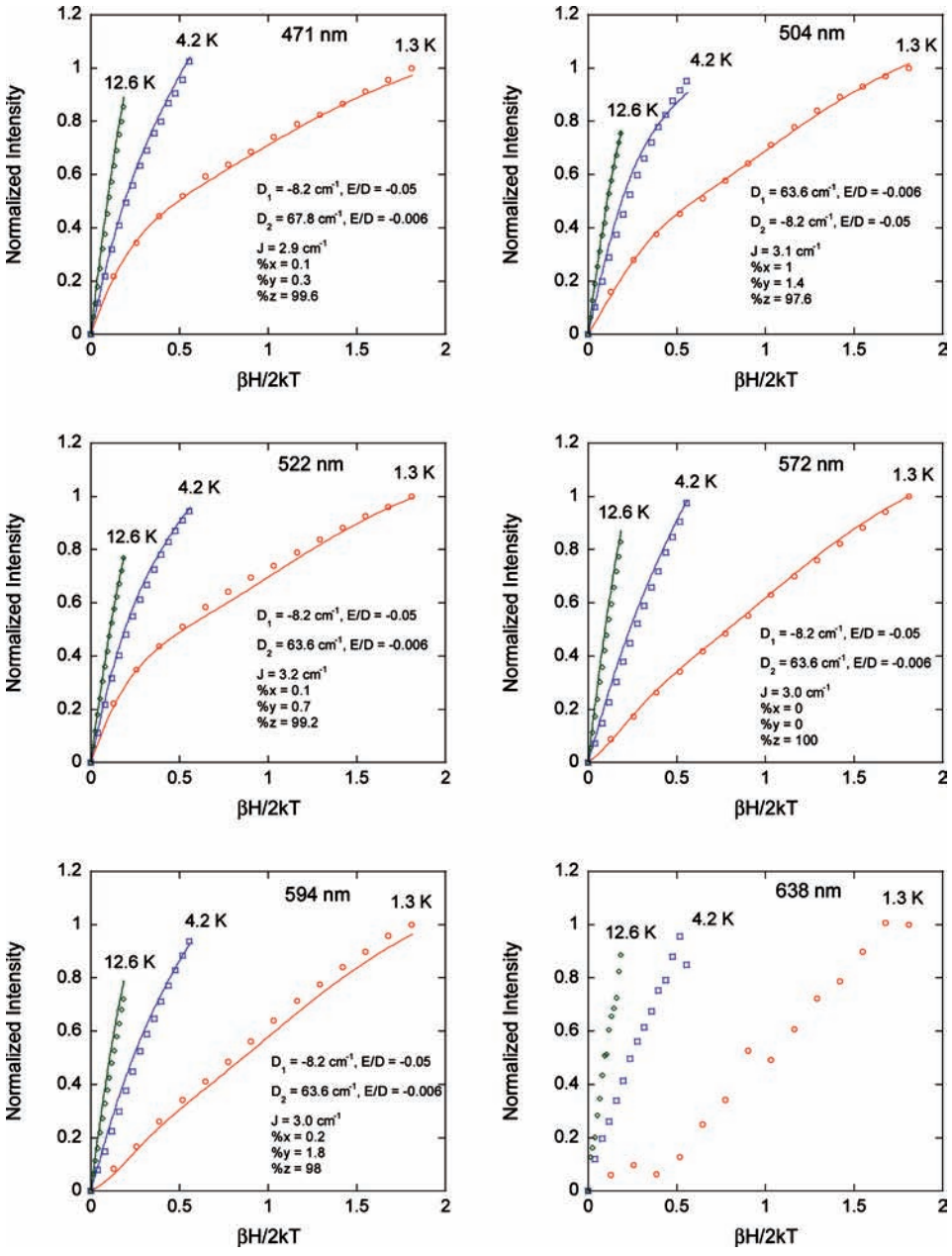

Figure 2. Magnetization plots for each band in the MCD spectrum of the complex. Lines represent the best fits using the dimer model. The 638 nm data were not fitted. Error bars (5% relative) are omitted for clarity; however, the calculated lines fall well within these error bars in all cases.

Gaussian peaks that had (nearly) the same band centers as found in the MCD spectrum, within a reasonable variation arising from spectral resolution limitations. However the bandwidths in the fitted absorption spectrum do not match those in the MCD spectrum for the reasons given above. These Gaussians are shown in Figure 1 in red and are listed in Table 1. The absorption spectrum required an additional three Gaussian peaks at 350, 388, and 419 nm to be fitted accurately. Since these peaks do not appear in the MCD spectrum, they can be attributed to ligand- and/or solvent-centered transitions. When the absorption spectrum is resolved in this way, it is apparent that the sharp, intense band at 504 nm in the MCD spectrum makes almost no contribution to absorption intensity. It is also clear that the moderately intense transitions at 471, 522, and 572 nm in the MCD spectrum are responsible for the bulk of the intensity in the absorption spectrum (Figure 1 and Table 1). The intensity reversal between the MCD and absorption spectra strongly suggests that the transitions at 471, 522, and 572 nm in the MCD spectrum arise from the 5-coordinate Co^{II} center and that the transition at 504 nm arises from the 6-coordinate Co^{II} center. A number of spectroscopic studies on mononuclear 5- and 6-coordinate Co^{II} complexes and on dinuclear 6-coordinate Co^{II} complexes support these assignments.[13,17,18,35,36] These assignments are further substantiated by AOM calculations, which are summarized in Table 1. The ε_σ values for 6- and 5-coordinate Co(II) complexes are typically between 3500 and 5500 cm^{-1} for N-donor ligands and between 2500 and 3500 cm^{-1} for O-donor ligands.[33d,e] The ε_σ values for the TMEDA N

(36) Lever, A. B. P. *Inorganic Electronic Spectroscopy*, 2nd ed.; Elsevier: Amsterdam, 1984; pp 480−505.

and OH^- ligands are high. This may be the result neglecting π-bonding for OH^- and the carboxylate ligands.

Analysis of the VTVH MCD. The magnetization plots for six of the observed MCD bands are shown in Figure 2. The magnetization plot for the 504 nm band is the only one from 6-coordinate Co^{II}; the others are from the 5-coordinate Co^{II}. What is immediately apparent is that the general shapes of the magnetization curves are similar for all the bands, suggesting that these transitions are similarly polarized and arise from the same ground state.

The first magnetization plot to be analyzed is that from the 504 nm band produced by 6-coordinate Co^{II}. Magnetically isolated, high-spin, 6-coordinate Co^{II} invariably produces magnetization plots that are characteristic of isolated, pseudo-Kramers doublet ground states; that is, the isotherms in the magnetization plots overlay one another or nearly do. We have shown this to be the case for several examples.[12,13,35] The primary reason is that high-spin 6-coordinate Co^{II} has a large zero-field splitting, $D > 40$ cm^{-1}, that creates an isolated doublet ground state, the only state populated at low temperatures in magnetically isolated Co^{II}. If the transition is *xy*-polarized, the low-temperature VTVH MCD data can often be fitted with a simple hyperbolic tangent function with an effective *g* between 4 and 6.[12] This is the case for hexaaquacobalt(II), for example (unpublished data), and is definitely not the case for the 504 nm band in this model complex. Furthermore, the initial steepness of magnetization plots suggests a ground state with a large effective *g* greater than 6,[37] which can happen only if the two cobalt ions are ferromagnetically coupled. The data could not be successfully fitted either to an isolated doublet ground state using the singlets/doublet model or to the monomer model. Thus, the magnetization data from the 504 nm band were fitted using a ferromagnetically coupled dimer model. The fits to the data are shown as the solid lines in Figure 2. The fit was not very sensitive to the axial zero field splitting (ZFS) parameter, *D*, for the 6-coordinate Co^{II} as long as *D* was greater than 40 cm^{-1}; however, the fit was very sensitive to both the magnitude and sign of *D* for the 5-coordinate Co^{II}. The fit was also very sensitive to the polarization, and a good fit was only possible with a predominantly *z*-polarized transition. Finally, the fit was moderately sensitive to the magnitude of the coupling constant, *J* (see below), but a positive *J* was required to achieve a good fit. Lastly, chi-squared for the fit was reduced by a factor of 3 if a small rhombic ZFS, *E*, was allowed.

The VTVH MCD data from the 5-coordinate Co^{II} were successfully fitted to a ferromagnetically coupled ground state. First, using the singlets and doublets model, an attempt was made to fit the magnetization data from the 5-coordinate MCD bands at 471, 522, 572, and 594 nm to a ground state for a magnetically isolated high-spin 5-coordinate Co^{II}, which is based on a ^4A ground term that is split into two doublets by ZFS ($D = -15$ to 30 cm^{-1}; a negative ZFS indicates that the $M_s = \pm 3/2$ is the lower doublet, and a positive ZFD indicates that the $M_s = \pm 1/2$ doublet is the lower one). The data could not be satisfactorily fitted using only two doublets. The data could not be successfully fitted with the monomer model, either. However, excellent fits were obtained using the dimer model with ferromagnetic coupling, *J* ranging from 2.9 to 3.2 cm^{-1}, and the same values for *D* and *E* as obtained in the 6-coordinate data fit, as indicated in Figure 2. The best fits were obtained using the 504 and 471 nm data because these were the best resolved MCD bands. Note that when fitting VTVH MCD data using the dimer model program, the subscript refers to the metal from which the transition arises. Thus D_1 and E_1 are the ZFS parameters for the 5-coordinate Co^{II} when fitting the VTVH data for the 471, 522, 572, and 594 nm bands, and D_1 and E_1 are the ZFS parameters for the 6-coordinate Co^{II} when fitting VTVH data for the 504 nm band.

The coupling constant and ZFS parameters determined for the model complex are used to calculate the energy, dimer ZFS, δ (levels with non-zero M_s will be split by $\pm\delta$), and spin of the 16 levels of the ground-state manifold (Table 2). Levels with a non-zero M_s are doublets, which can give rise to C-term and B-term MCD, and those with a zero M_s are singlets, which can give rise to only B-term MCD. There are three doublets and one singlet at energies of 26 cm^{-1} or below that can be thermally populated at low temperatures (25 K and below). Thus the low-temperature VTVH MCD data were fitted, using the singlets and doublets model, to three doublets and one singlet. The fits and parameters are shown in Supporting Information, Figure S3, and the fits to the experimental data are nearly perfect, as might be expected

Table 2. Energy Levels and Spin States for the 16 Sublevels in the Ground State[a]

average energy [cm^{-1}][b]	δ [cm^{-1}]	S_{total}, $\lvert M_{s\ total}\rvert$[c]
0.01	0.01	3,2
2.98	1.27	3,1
10.46	0	3,0
26.00	1.48	2,1
34.53	0	2,0
118.7	0	3,3
144.6	0.13	2,2
146.9	0	1,0
146.9	0	0,0
154.2	0.21	1,1

[a] For $J = 3.0$ cm^{-1}, $D_1 = -8.2$ cm^{-1}, $E_1/D_1 = -0.05$, $D_2 = 63.6$ cm^{-1}, $E_2/D_2 = -0.006$. [b] In the case of doublets, average energy is the average of the two levels split by δ. [c] In zero field levels with non-zero M_s will be split by $\pm\delta$.

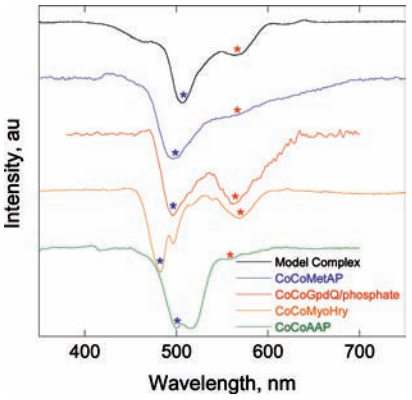

Figure 3. Comparison of the MCD spectrum of the model complex to those of four dicobalt(II)-substituted proteins. The diagnostic 6-coordinate (blue asterisk) and 5-coordinate (red asterisk) bands are indicated. The data have been normalized to the major 6-coordinate band.

(37) Johnson, M. K. In *Physical Methods in Bioinorganic Chemistry*; Que, L., Jr., Ed.; University Science Books: Sausalito, CA, 2000; Chapter 5.

Table 3. Summary of Magnetic Coupling Constants in Enzymes and Related Complexes

bridging core	Co···Co [Å]	Co−O−Co [deg]	J^a [cm^{-1}]	reference
$Co_2(\mu\text{-OH})(\mu\text{-Ph}_4\text{DBA})$	3.262	104	3.0	32, this work
Co_2AAP, $Co_2(\mu\text{-OH})(\mu\text{-1,3-O}_2\text{CCH}_3)$	3.3	unknown	3.4	39, this work
Co_2MyoHry, $Co_2(\mu\text{-OH})(\mu\text{-1,3-O}_2\text{CCH}_3)_2$	3.54[b]	unknown	3.4	42, this work
$Co_2(\mu\text{-OH})(\mu\text{-1,3-O}_2\text{CCH}_3)_2$	3.435	121.3	1.7	13,31
MetAP/F,$Co_2(\mu\text{-OH(H)})(\mu\text{-1,3-O}_2\text{CR})_2$	3.1[c]	84[c]	2.9	13
MetAP,$Co_2(\mu\text{-OH}_2)(\mu\text{-1,3-O}_2\text{CR})_2$	3.2	98	≈0	13
$Co_2(\mu\text{-OH}_2)(\mu\text{-1,3-O}_2\text{CCH}_3)_2$	3.548	113	−0.2	25
$Co_2(\mu\text{-OH}_2)(\mu\text{-1,3-O}_2\text{CCH}_3)_2$	3.687	117	−1.6	26,27
$Co_2(\mu\text{-OH}_2)(\mu\text{-1,3-O}_2\text{CCH}_3)_2$	3.597	115	−0.7	28,29
$Co_2(\mu\text{-OH}_2)(\mu\text{-1,3-O}_2\text{CCCl}_3)_2$	3.696	116	−1[d]	30

[a] These are all based on a Hamiltonian using $-2JS_1 \cdot S_2$. [b] Determined from the EXAFS of Co(II)-substituted Hry. [c] Assumed from the structure of CoCo*Hs*MetAP/F, PDB:1BOA. [d] Estimated from Néel temperature of 4.3 K.

for the large number of parameters required in this type of fit. Notably, however, fitting the VTVH MCD data for all the bands required a large effective g for the ground-state doublet, consistent with ferromagnetic coupling.

Discussion

This study of the mixed 5- and 6-coordinate dicobalt(II) complex shows that it is an excellent spectroscopic model for several dicobalt(II)-substituted enzymes and proteins. In particular, the qualitative and quantitative features of the MCD spectrum of the model complex match those of dicobalt(II)-substituted GpdQ, MetAP, AAP, and myohemerythrin (Figure 3). These results support some previous conclusions, and in other cases, enable those conclusions to be reinterpreted or clarified.

The MCD spectrum of the dicobalt(II) form of GpdQ shows two major negative C-term bands, at 495 and 574 nm (564 nm in the presence of phosphate), which have been assigned to 6- and 5-coordinate Co^{II}, repectively.[6] An early crystal structure of CoCoGpdQ (dicobalt(II)-substituted glcerophosphodiesterase from *Enterobacter aerogenes*) was unable to pinpoint the exact number of water ligands to the metals; thus, these assignments were based on ligand field arguments. These tentative values are now confirmed by both these results on the model complex and a higher resolution crystal structure.[6] A more important result of the MCD study of CoCoGpdQ was that it enabled us to determine that the 6-coordinate metal binding site had higher binding affinity than the 5-coordinate site. This finding was possible only because 5- and 6-coordinate Co(II) are easily distinguished in the low temperature MCD spectrum, as this study demonstrates.

The MCD[12,13] and absorption spectra[9,12] of dicobalt(II) MetAP are remarkably similar to those of this model complex. The absorption spectrum of CoCoMetAP (dicobalt(II)-substituted methionine aminopeptidase from *Escherichia coli*) has four maxima, all due to 5-coordinate Co^{II} at 526, 571, 629, and 685 nm. The intensity from 5-coordinate Co^{II} is dominant in the absorption spectrum, as it is in the model complex. On the other hand, in the low-temperature MCD spectrum, bands are observed at 472 and 495 nm, arising from 6-coordinate Co^{II}, in addition to bands at 567 and 625 nm from the 5-coordinate Co^{II}. MetAP, like GpdQ, has large differential metal binding constants.[9−11] However, in MetAP the 5-coordinate site has tighter metal binding, a finding confirmed in an MCD study.[12]

The 1.3 K MCD spectrum of dicobalt(II)-substituted AAP (CoCoAAP, dicobalt(II)-substituted aminopeptidase from *Aeromonas proteolytica*) also shows a band at 497 nm, attributable to 6-coordinate Co^{II}, and bands at 480, 519, 555, and 583 attributable to 5-coordinate Co^{II} (see Supporting Information). This spectrum also is very similar to that of the model complex. The MCD spectrum of CoCoAAP taken at 250 K still shows all of these bands (Supporting Information, Figure S4), but the relative intensities of the 5- and 6-coordinate bands change dramatically, which is the reason that the room-temperature MCD, first described in 1985, is dominated by the 5-coordinate bands.[41] Analysis of the VTVH MCD data from the 497 and 519 nm bands of CoCoAAP is also consistent with a mixed 5- and 6-coordinate active site (Supporting Information, Figure S5). The exact ligation of the Co^{II} ions in CoCoAAP is controversial, but the mixed 5- and 6-coordinate interpretation is consistent with the latest X-ray crystallography study.[39]

A final example is the low-temperature MCD spectrum of dicobalt(II)-substituted myohemerythrin (CoCoMyoHry, dicobalt(II)-substituted myohemerythrin from *Themiste zostericola*).[43] Bands at 445 and 481 nm have been attributed to 6-coordinate Co^{II}, and bands at 511, 569, 593, and 622 have been attributed to 5-coordinate Co^{II}.[43] The MCD spectrum of CoCoMyoHry, shown in Supporting Information, Figure S6, is remarkably similar to that of the model complex. The analysis of the VTVH MCD data from the 481 and 569 nm bands supports a mixed 5- and 6-coordinate active site, and this result is consistent with an EXAFS study of cobalt(II)-substituted hemerythrin from *Phascolopsis gouldii*.[42]

Our hope has been that the ground-state parameters of coupled dicobalt(II) enzyme active sites could provide some insight or biologically relevant information. In particular, the sign and magnitude of the coupling constant, J, has been proposed as a possible indicator of the nature of the single-atom bridging ligand, be it water, hydroxide, or oxide.[26] Many proposed dimetallic hydrolase mechanisms employ the bridging water or hydroxide as the attacking nucleophile.[1−3] In crystal structures of these enzymes, being certain of the exact state of protonation of this bridging ligand is often not

(38) Desmarais, W.; Bienvenue, D. L.; Bzymek, K. P.; Petsko, G. A.; Ringe, D.; Holz, G. A. *J. Biol. Inorg. Chem.* **2006**, *11*, 398–408.
(39) Munih, P.; Moulin, A.; Stamper, C. C.; Bennett, B.; Ringe, D.; Petsko, G. A.; Holz, R. C. *J. Inorg. Biochem.* **2007**, *101*, 1099–1107.
(40) Bennett, B.; Holz, R. C. *Biochemistry* **1997**, *36*, 9837–9846.
(41) Prescott, J. M.; Wagner, F. W.; Holmquist, B.; Vallee, B. L. *Biochemistry* **1985**, *24*, 5350–5356.
(42) Zhang, J.-H.; Kurtz, D. M.; Maroney, M. J.; Whitehead, J. P. *Inorg. Chem.* **1992**, *31*, 1359–1366.
(43) Martins, L. J. *Studies on the Coordination Chemistry of Myohemerythrin*, PhD dissertation, University of Utah, **1994**.

possible, and MCD spectroscopy may be able to provide some answers. In Table 3 we have listed every dicobalt(II) complex or enzyme active site with a bridging water or hydroxide, as well as an additional bridging carboxylate or two that have a reported *J*. This is not a long list, but the trend is quite clear. The μ-hydroxo structures are ferromagnetically coupled, whereas the μ-aqua structures are either not coupled or weakly antiferromagnetically coupled. We are assuming that CoCoAAP has a μ-hydroxo because the 0.95 Å resolution crystal structure of ZnZnAAP has been interpreted as having a likely μ-hydroxo bridge,[38] and the hydrolysis products (pK_h for $M^{2+} + H_2O = MOH^+ + H^+$) are similar for Zn^{II} and Co^{II} at 9.3 and 9.8, respectively.[45]

Conclusions

The [Co_2(μ-OH)(μ-Ph_4DBA)$(TMEDA)_2$(OTf)] complex is an excellent spectroscopic model for dicobalt(II)-substituted protein active sites that have one 5- and one 6-coordinate metal binding site. The MCD spectrum has resolved d-d transitions associated with each Co^{II} ion, and these results enable confident assignment of the corresponding MCD bands in the proteins. Determination that Co^{II} ions are ferromagnetically coupled in the model complex, as they are in other μ-hydroxo model complexes and enzyme active sites, suggests the possibility that *J* could be used to distinguish μ-aqua and μ-hydroxo bridging motifs in dicobalt(II) systems.

Acknowledgment. The authors acknowledge the National Science Foundation for financial support: Grant NSF/RUI CHE0554083 and Grant NSF/MRI CHE0820965. A.S.V. also acknowledges the National Institutes of Health and the National Center for Research Resources for financial support through a Vermont Genetics Network grant. The authors also gratefully acknowledge Professor Jeffrey H. Byers of Middlebury College for assistance with the organic synthesis steps.

Supporting Information Available: Equations used in the dimer and singlets/doublets fitting programs; additional MCD spectra of [Co_2(μ-OH)(μ-Ph_4DBA)$(TMEDA)_2$(OTf)] taken at temperatures from 1.3 to 50 K; MCD and diffuse reflectance spectra of solid [Co_2(μ-OH)(μ-Ph_4DBA)$(TMEDA)_2$(OTf)]; singlets/doublets model fitting results on [Co_2(μ-OH)-(μ-Ph_4DBA)$(TMEDA)_2$(OTf)]; MCD spectra, magnetization data, and dimer model fits of CoCoAAP; and MCD spectra, magnetization data, and dimer model fits of CoCoMyoHry. This material is available free of charge via the Internet at http://pubs.acs.org.

(44) Martins, L. J.; Hill, C. P.; Ellis, W. R. *Biochemistry* **1997**, *36*, 7044–7049.

(45) Baes, C. F.; Mesmer, R. E. *The Hydrolysis of Cations*; Krieger: Malabar, FL, 1986; pp 238, 288.